pH Studies on the Mechanism of the Pyridoxal Phosphate-Dependent Dialkylglycine Decarboxylase†

Xianzhi Zhou and Michael D. Toney*

Department of Biochemistry, Albert Einstein College of Medicine, Bronx, NY 10461

Received June 18, 1998; Revised Manuscript Received September 30, 1998

ABSTRACT: The pH dependence of the steady-state kinetic parameters for the dialkylglycine decarboxylase-catalyzed decarboxylation-dependent transamination between 2-aminoisobutyrate (AIB) and pyruvate is presented. The pH dependence of methylation and DTNB modification reactions, and spectroscopic properties, is used to augment the assignment of the kinetic pK_a's to specific ionizations. The coincidence of pK_a values (∼7.4) observed in k_{cat}/K_{AIB}, $1/K_{AIB}$, K_{is} for pyruvate, K_{PLP}, and in absorbance and fluorescence titrations demonstrates that AIB is not a sticky substrate. It furthermore suggests that the decarboxylation step, or a conformational isomerization preceding it, limits the rate of the overall catalytic cycle. Coexisting, kinetically distinguishable conformers of DGD-PLP, originating from an alkali metal ion binding site, were previously demonstrated at pH 8.2 for DGD-PLP (Zhou, X., Toney, M. D. *Biochemistry 37*, 5761−5769). The pK_a value of ∼8.8 observed in k_{cat}, k_{cat}/K_{AIB}, K_d for K^+, spectrometric titrations, and the reaction of DGD-PLP with DTNB is tentatively assigned to the conformational change interconverting the two enzyme forms previously characterized. Three pK_a's are observed in pH titrations of the DGD-PLP coenzyme absorbance. Individual spectra for the four ionization states are deconvoluted by fitting log-normal curves. All four ionization states have both ketoenamine and enolimine tautomers present. This and a review of spectral data in the literature lead to the conclusion that the pK_a of ∼7.4, which gives the largest spectral changes and controls k_{cat}/K_{AIB}, is not deprotonation of the aldimine nitrogen. Rather, it must be an active site residue whose ionization alters the ratio between ketoenamine and enolimine tautomers.

Dialkylglycine decarboxylase is an unusual PLP-dependent[1] enzyme that catalyzes both decarboxylation and transamination half-reactions in its ping-pong catalytic cycle. Details of the mechanism are shown in Scheme 1. The first half-reaction is an oxidative decarboxylation. The external aldimine is formed from the internal aldimine by a transimination reaction where the substrate α-amino group replaces the ϵ-amino group of Lys272 in the aldimine linkage to PLP. Loss of CO_2 gives the quinonoid, which goes forward to the ketimine via protonation at C4′. Hydrolysis of the ketimine completes the decarboxylation half-reaction, yielding DGD-PMP and a ketone. The catalytic cycle is completed by a classical transamination half-reaction between DGD-PMP and an α-keto acid (preferably pyruvate), regenerating the aldehyde form of the coenzyme and giving an L-amino acid product.

The crystal structure (*1*, *2*) shows several potentially ionizable groups in the active site, including those on the coenzyme (e.g., pyridine nitrogen, aldimine nitrogen, phosphate ester). The pyridine nitrogen of PLP makes a hydrogen bond with the side-chain carboxylate of Asp243. The phenolic 3′-hydroxyl group of PLP is assumed to be ionized and receives hydrogen bonds from the side-chain amide nitrogen of Gln246, the protonated Schiff base of the external aldimine, and an active site bound water molecule. The phosphate ester on C5′ is involved in a total of nine hydrogen bonds; five are from well-ordered water molecules and four others originate from the main-chain amides of Gly111, Ala112, and Thr303, as well as the hydroxyl group of the latter. A hypothetical model of the external aldimine of isovaline (*2*) suggests that the substrate carboxylate group accepts three hydrogen bonds from the side-chains of Lys272, Gln52, and Arg406. Finally, DGD has an alkali metal ion binding site near the active site that also contains ionizable residues. Potassium at this site activates the enzyme, while sodium inhibits it (*3*, *4*).

This study presents a detailed investigation of the pH dependence of the steady-state kinetic parameters for the DGD-catalyzed decarboxylation-dependent transamination reaction between AIB and pyruvate, including its inhibition by pyruvate. Additional extra-kinetic methods have also been employed to provide independent support for the assignment of the observed pK_a values to specific groups. For example, absorbance and fluorescence titrations of enzyme-bound

† Supported by grant GM54779 from the National Institutes of Health.

* To whom correspondence should be addressed: Address: 1300 Morris Park Ave., Bronx, NY 10461. Tel: 718-430-2347. E-mail: toney@aecom.yu.edu.

[1] Abbreviations: DGD, dialkylglycine decarboxylase; PLP, pyridoxal phosphate; PMP, pyridoxamine phosphate; DGD-PLP, PLP form of DGD; DGD-PMP, PMP form of DGD; IANBD, *N*-((2-(iodoacetoxy)-ethyl)-*N*-methyl)amino-nitrobenz-2-oxa-1,3-diazole; AIB, 2-aminoisobutyrate; pyr, pyruvate; 2°ADH, NADP-dependent secondary alcohol dehydrogenase; ADA, *N*-[2-Acetamido]-2-iminodiacetic acid; TEA, triethanolamine; bicine, *N*,*N*-bis[2-hydroxyethyl]glycine; Bis-tris propane, 1,3-bis[tris(hydroxymethyl)-methylamino]propane; TMA, tetramethylammonium ion; DTNB, dithio-bis(nitrobenzoic acid).

10.1021/bi981455s CCC: $18.00
Published on Web 12/11/1998

Scheme 1

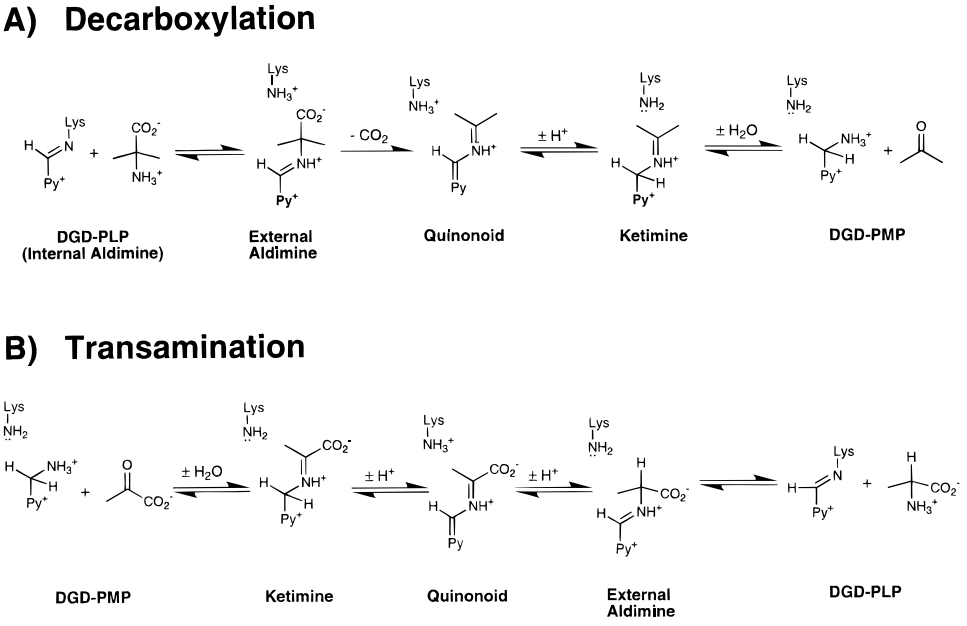

coenzyme and chemical modification studies are presented. A generally consistent picture of the kinetically significant ionizations is constructed.

EXPERIMENTAL PROCEDURES

Materials. AIB, pyruvic acid, PLP, 2°ADH, and NADPH were purchased from Sigma. Succinic acid, potassium hydroxide, DTNB, ADA (*N*-[2-Acetamido]-2-iminodiacetic acid), TEA (triethanolamine), bicine (*N*,*N*-bis[2-hydroxyethyl]glycine), and Bis-tris propane (1,3-bis[tris(hydroxymethyl)-methylamino]propane) were from Aldrich. IANBD was from Molecular Probes.

Initial Velocity Studies. A Kontron UVIKON 9420 spectrophotometer was used. The reaction was followed by coupling the acetone produced from AIB to the 2°ADH reaction and monitoring the decrease in NADPH absorbance at 340 nm. Reaction mixtures for the determination of initial velocities contained 30 mM buffer, 0.2 mM NADPH, 1 unit/mL 2°ADH, 100 mM dipotassium succinate, 10 mM disodium succinate, 500 μM PLP, and varying concentrations of AIB and pyruvate. Pyruvate was obtained as the free acid and titrated with TMA hydroxide so that constant concentrations of alkali metal ions were maintained.

The steady-state kinetic parameters (k_{cat}, k_{cat}/K_{AIB}, k_{cat}/K_{pyr}, and K_i's) were determined by measuring initial rates for a 6 × 6 matrix of AIB and pyruvate concentrations at each pH. The following buffers, covering the pH range from 5.5 to 9.5, were employed: succinate (pH 5.5−6.0), ADA (pH 5.9−7.3), TEA (pH 7.2−8.3), bicine (pH 7.8−8.8), and Bis-tris propane (pH 8.5−9.5). All buffers were titrated to the appropriate pH with either TMA hydroxide (succinate, ADA, bicine) or phosphoric acid (TEA, Bis-Tris propane). Overlaps between buffers were made when they were changed to ensure against specific buffer effects. The pH's of the reaction mixtures were measured after initial rates were obtained. Ionic strength was monitored by the conductivity of reaction mixtures and did not vary significantly under the conditions employed.

The concentration of 2°ADH required to give true initial velocities (as shown by linear velocity versus enzyme concentration plots) of the DGD reaction with no detectable lag time was determined at pH's 6.0, 7.8, and 9.4. A single concentration sufficient for the entire range (1 unit/mL) was used throughout. A single DGD concentration (4.0×10^{-8} M) within the linear range of each of these pH values was used for the entire pH range. The required substrate concentrations were estimated for each pH value from the K_M values at the previous pH. Concentrations generally ranged from $0.2K_M$ to $5K_M$.

pH Profile Curve Fitting. The initial rate data for the pH profiles were fitted to eq 1, which describes a ping-pong bi bi kinetic mechanism with noncompetitive substrate inhibition. The program GraFit (Erithacus Software) was used with simple, robust weighting for all curve fitting.

$$v = V_{max}[AIB][pyr]/\{(K_b[AIB] + [AIB][pyr])(1 + [pyr]/K_{ii}) + K_a[pyr](1 + [pyr]/K_{is})\} \quad (1)$$

Here, K_a stands for K_{AIB}, K_b for K_{pyr}, K_{is} for competitive inhibition constant for DGD-PLP by pyruvate, and K_{ii} for the uncompetitive inhibition constant. An F-test demonstrated that eq 1 fits the data significantly better than the equation describing purely competitive inhibition (>99% confidence). The initial rate data were also fitted to an equation similar to eq 1 but including a second enzyme form (*4*). The pK_a values obtained from these fits were similar to those obtained from eq 1 except with larger errors. The 6 × 6 matrixes did not contain enough information to define well the larger number of parameters. The values presented here are from fits of the initial rate data to eq 1.

The pH dependences of k_{cat} and $1/K_{is}$ were fitted to a bell-shaped curve with limits of 0 at both pH extremes (eq 2).

$$y = \frac{\text{limit}}{10^{(pH-pK_2)} + 10^{(pK_1-pH)} + 1} \quad (2)$$

The k_{cat}/K_{AIB} data were fitted to a similar equation with a

nonzero high pH limit. The fit of an equation describing a single ionization to the k_{cat}/K_{AIB} data was significantly worse as determined by an F-test (>99% confidence).

The pH dependence of k_{cat}/K_{pyr} fits best to an equation with a single pK_a with one active species and zero activity at high pH (eq 3).

$$y = \frac{\text{limit}}{10^{(\text{pH}-\text{p}K_a)} + 1} \quad (3)$$

The pH dependence of $1/K_{AIB}$ was fitted to eq 3 except that the pH and pK_a variables were exchanged.

pH Dependence of PLP binding. Each assay contained 40 mM AIB, 2 mM pyruvate-TMA, 0.2 mM NADPH, 1 unit/mL 2° ADH, and 100 mM potassium succinate. The buffers and pH ranges for their use were the same as those given above. PLP concentrations were varied from 0 to 500 μM. DGD (67 nM) was incubated in the reaction mixture lacking AIB and pyruvate for 1 h. The reactions were initiated by the addition of substrates. The initial rate versus [PLP] data were fitted to a simple Michaelis−Menten equation to obtain estimates for K_{PLP}.

The K_{PLP} versus pH data were fitted to an inverse bell-shaped curve (eq 4).

$$y = \frac{\text{low} + \text{limit}(10^{(\text{pH}-\text{p}K_a)})}{10^{(\text{pH}-\text{p}K_a)} + 1} \quad (4)$$

pH Dependence of Potassium Binding. The rate of K^+ dissociation from DGD-PLP was measured by the change in activity versus time with the K^+ form of DGD-PLP. The assay conditions were 40 mM TEA-HCl, pH 7.9, 500 μM PLP, 100 mM $(TMA)_2$ succinate containing 50 mM AIB, and 2 mM pyruvate-TMA. The rate of decrease of the initial rate yielded a half-life of ~1.2 min for K^+ dissociation. The association of K^+ with DGD-PLP (similarly measuring the change in initial rate versus time) in the presence of 2 mM K^+ has a half-life of ~1.3 min.

DGD-PLP was dialyzed against 40 mM TEA-HCl, pH 8.0, 500 μM PLP to remove potassium ions. Dialyzed enzyme was incubated with various concentrations of dipotassium succinate for 30 min and assayed for activity. The buffers and assay conditions used were the same as in the initial rate studies described above, except that 100 mM $(TMA)_2$ succinate was used to maintain ionic strength. The initial rate data were fitted to a Michaelis−Menten equation with an additional offset term to account for the residual activity of the metal-free enzyme (eq 5).

$$y = \frac{V_{max}[K^+]}{K_d + [K^+]} + \text{offset} \quad (5)$$

The K_d values for K^+ so obtained were fitted to an equation describing a single ionization involving multiple protons (eq 6).

$$y = \frac{\text{low} + \text{limit}(10^{n(\text{pH}-\text{p}K_a)} + 10^{(\text{pH}-\text{p}K_a)})}{1 + 10^{(\text{pH}-\text{p}K_a)} + 10^{n(\text{pH}-\text{p}K_a)}} \quad (6)$$

Here, n is the number of protons associated with the ionization.

Titration of AIB. AIB (0.1 M) was titrated with aliquots of 1 M KOH. Both solutions contained 100 mM K^+ succinate. The KOH volume versus pH data were fitted to eq 7.

$$y = \frac{\text{limit}(10^{(\text{pH}-\text{p}K_a)})}{1 + 10^{(\text{pH}-\text{p}K_a)}} + \text{offset} \quad (7)$$

Spectrophotometric pH Titration of DGD-PLP. DGD-PLP (~50 μM subunits) in 5 mM potassium borate pH 9.5, 100 mM potassium succinate, 10 μM PLP was prepared by multiple buffer changes in a Centricon-30 (Amicon) ultrafiltration device. Aliquots of 30 mM succinic acid were added to alter the pH. The pH intervals between scans were approximately 0.1 units. DGD begins to precipitate below pH 5.7. Absorbance spectra (250−550 nm) versus pH were collected on an HP 8453 diode array spectrophotometer in the pH range 5.7−9.5 and analyzed globally by Specfit (version 2.10, Spectrum Software Associates).

The calculated spectra for the individual species obtained from the global analysis were further analyzed by fitting sums of log-normal curves to them (*5*). The fitting was performed with the program Scientist (Micromath). The percentages of each species were calculated with the molar areas given by Metzler and Metzler (*5*).

Fluorescence pH Titration of IANBD-Labeled DGD-PLP. IANBD ester was used to label DGD. DGD-PLP (30 μM; 1 mL) was reacted with 200 μM IANBD ester in 50 mM TEA-HCl, pH 7.9, for 15 min in the dark. The reaction was stopped by adding DTT to a final concentration of 2 mM. The unreacted IANBD ester was washed out by five 1:10 concentration/redilution cycles using a Centricon-30 and 5 mM TEA-HCl, pH 7.9, 500 μM PLP. The final DGD solution (200 μL) was diluted with 5 mM potassium borate, pH 9.8, 100 mM potassium succinate, 500 μM PLP to give a final DGD concentration of 15 μM. The pH was adjusted by adding aliquots of 30 mM succinic acid. After each pH adjustment, a 5 min incubation was allowed before scanning. The excitation wavelength was 489 nm, and the emission scan was from 500 to 710 nm. The data were collected on an instrument from Photon Technologies and analyzed by Specfit.

Fluorescence pH Titration of DGD-PMP. Due to the relatively fast dissociation of PMP (half-life ~10 min at pH 8), individual enzyme samples were prepared (by reaction with an excess of AIB) at the appropriate pH values and scanned immediately after formation. Fluorescence emission spectra were taken from 350 to 550 nm with 330 nm excitation. The solution contained 2 μM DGD-PLP with 5 μM free PLP and 50 mM buffer. The scans were analyzed in Specfit by global fitting of spectra versus pH.

Dependence of DTNB Reaction on pH. The reactions were monitored using an Applied Photophysics SX17.MV stopped-flow spectrophotometer. One syringe contained 100 mM buffer, 100 mM dipotassium succinate, and 1.2 mg/mL DGD-PLP. The other contained an identical solution except that 20 mM DTNB replaced the enzyme. The reactions were followed for 100 s, and data points were logarithmically spaced. Data were measured in the pH range 8.1−9.4. The background hydrolysis of DTNB was significant under these conditions, so the data were fitted to an equation describing a double-exponential process with a linear background. The

amplitudes of the exponential processes were fitted either to eq 3 (fast phase) or to an equation describing a single ionization with a finite limit at low pH (slow phase).

Reductive Methylation of DGD-PMP as a Function of pH. Apo-DGD was prepared by adding an excess of AIB to DGD-PLP, followed by several buffer changes (TEA-HCl, pH 7.9, no metal ions) in a Centricon-30 to remove AIB and coenzyme. DGD-PMP was obtained by incubating 40 μM apoDGD with 5 mM PMP overnight. DGD-PMP (15 μM) was reacted with 10 mM sodium cyanoborohydride and 8 mM formaldehyde in either 100 mM potassium phosphate (pH 6−8) or 60 mM potassium pyrophosphate (pH 8−10). Aliquots (20 μL) of the reaction mixtures were removed at intervals and incubated in 1 mL reaction mixtures lacking pyruvate but containing 100 mM AIB and 100 μM PLP for ~2 min. The 2°ADH coupled assay was initiated by the addition of pyruvate. The rate constant for reductive methylation at each pH was obtained from fitting the activity versus time curve to a single-exponential model with an offset (eq 8).

$$\text{activity} = (a_i - a_f)e^{(-kt)} + a_f \qquad (8)$$

Here, a_i is the activity before methylation and a_f is the activity remaining after methylation is complete.

DGD-PMP was exhaustively methylated in potassium phosphate, pH 8.0. The buffer was exchanged to 50 mM TEA-HCl, pH 7.9, with 100 μM PLP by concentration/redilution. Dipotassium succinate (100 mM final) was added, and the mixture was incubated for 2 h. The CD spectrum (Jasco J-720) and activity of this reconstituted DGD were measured.

RESULTS

Initial Velocity Studies. Double-reciprocal plots for the DGD-catalyzed reaction between AIB and pyruvate over a wide range of substrate concentrations are shown in Figure 1A. The kinetic mechanism of DGD is known from previous studies (*6, 7*) to be ping-pong. Figure 1A shows parallel lines only at low concentrations of pyruvate. At concentrations of 5 mM and higher, the value of k_{cat}/K_M decreases with increasing pyruvate concentration, suggesting that substrate inhibition by pyruvate occurs as previously observed (*6, 7*). This is demonstrated by the upturn at high pyruvate concentrations in Figure 1B. The data require a noncompetitive inhibition equation to account fully for the data. Inhibition of the coupling enzyme by pyruvate at these concentrations was not observed over the entire pH range. The data in Figure 1 yield the following parameters: $k_{cat} = 17.7 \pm 0.5\ s^{-1}$, $K_{pyr} = 0.098 \pm 0.008$ mM, and $K_{AIB} = 2.2 \pm 0.2$ mM.

pH Profiles for the Steady-State Kinetic Parameters. The pH dependence of k_{cat} for the AIB/pyruvate reaction is shown in Figure 2A. The data fit best to a bell-shaped curve with minima of 0 at both pH extremes. The k_{cat} values decrease below a pK_a of 5.9 and above a pK_a of 8.7 (Table 1).

Figure 2B shows the pH dependence of k_{cat}/K_{AIB}. These data fit best to a bell-shaped curve with a nonzero minimum at high pH. The value of the acidic pK_a is 7.3, coincident with that observed in the spectrophotometric pH titration of DGD-PLP (Table 1, see below). The higher pK_a value (9.1) is not the same as that for free AIB (10.1) under identical conditions (Table 1). However, this pK_a coincides approximately with the basic pK_a's observed in both the k_{cat} pH profile and the spectrophotometric titration of DGD-PLP (Table 1).

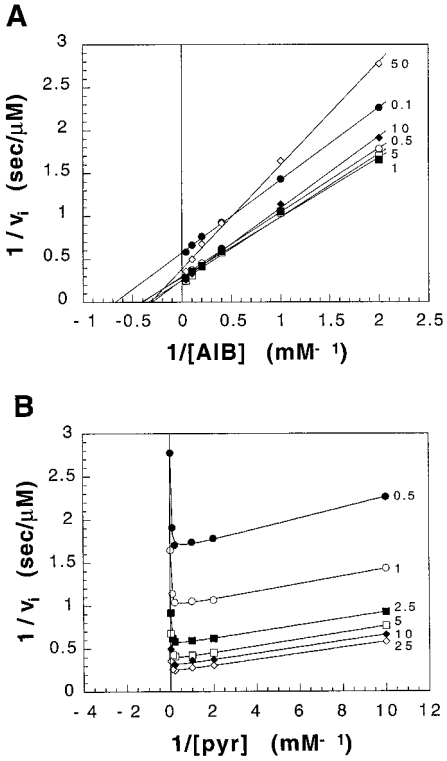

FIGURE 1: (A) Double-reciprocal plot for AIB in the decarboxylation-dependent transamination reaction between AIB and pyruvate. (B) Double-reciprocal plot for pyruvate. The lack of parallelism in A and the upward curvature in B demonstrate substrate inhibition by pyruvate. Numbers to the right of the lines indicate the concentration of the second substrate. Reactions were performed at pH 7.5 under the buffer conditions described in Experimental Procedures. The data fit best to a noncompetitive inhibition equation (eq 1) as compared to a purely competitive inhibition equation as determined by an F-test ($p < 0.005$).

Only one pK_a is observed in the k_{cat}/K_{pyr} pH profile (Figure 2C). This parameter decreases at higher pH values with a pK_a of 7.8 (Table 1). The data fit best with a 0 high pH limit. This pK_a value matches the lower pK_a observed in the fluorescence titration of DGD-PMP (see below).

The pH dependence $1/K_{AIB}$ (Figure 3) yields a pK_a value of 7.5 ± 0.1. This value is approximately the same as that observed in the k_{cat}/K_{AIB} and K_{is} profiles as well as in the spectrophotometric pH titrations (see below).

The pH dependence of the pyruvate $1/K_{is}$ fits reasonably well to a bell-shaped curve going to 0 at the pH extremes, although the data at high pH show significant scatter and the high pH extreme may be nonzero. This ambiguity could not be resolved by curve fitting. The fitted pH-independent limit of K_{is} is 10 mM. The value of the acidic pK_a is 6.3, close to the lowest pK_a (6.0) observed in the spectrophotometric titration of DGD-PLP (Table 1). The basic pK_a (7.6) coincides with the middle pK_a observed in the spectrophotometric titration of DGD-PLP and with the acidic pK_a observed in the k_{cat}/K_{AIB} profile.

The pyruvate K_{ii} is independent of pH from at least pH 5.5 to pH 9.0. The average value of K_{ii} is 108 ± 16 mM in the pH range measured.

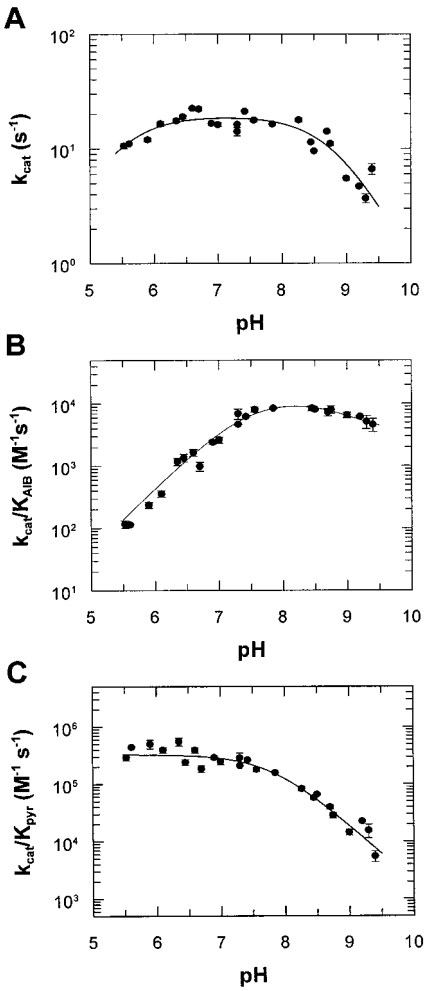

FIGURE 2: (A) The pH dependence of k_{cat} for the AIB/pyruvate reaction. The pK_a values are 5.9 ± 0.1 and 8.7 ± 0.1. The pH-independent value of k_{cat} is 17.8 ± 0.4 s^{-1}. (B) The pH dependence of k_{cat}/K_{AIB}. The pK_a values are 7.3 ± 0.1 and 9.1 ± 0.1. (C) The pH dependence of k_{cat}/K_{pyr}. The pK_a value is 7.8 ± 0.1.

pH Profile for K_{PLP}. The pH dependence of K_{PLP} fits best to an inverse bell-shaped curve. PLP binds to DGD with highest affinity at neutral pH values. The best-fit limiting value of K_{PLP} is ~2 μM.

pH Dependence of Metal Ion Binding. The pH dependence of the activation of DGD-PLP by potassium in the presence of high PLP concentrations was studied to determine the pK_a's controlling metal ion binding and also to determine the concentration of potassium needed to maintain the enzyme saturated over the entire pH range studied. The data fit best to an equation describing a single ionization with multiple protons associated with it (eq 6). The fitted value for the pK_a is 8.8, while the value for the number of protons is 1.7 ± 0.4. The fit to an equation describing a single ionization with a single proton is significantly worse as determined by an F-test (94% confidence).

DTNB pH Profile. The reaction of 10 mM DTNB with DGD-PLP occurs in two kinetic process. The rate constants for these increase linearly with hydroxide concentration. The amplitudes on the other hand show more complex pH dependence. The amplitude for the fast phase initially increases and then decreases in the pH range examined (Figure 4A). The slow phase amplitude shows a monotonic increase with pH (Figure 4B). The pK_a values extracted from the amplitude data are 8.2 and 8.7 for the fast phase and 8.80 for the slow (Table 1).

pH Profiles for Reductive Methylation of DGD-PMP. DGD-PMP was reductively methylated with formaldehyde and sodium cyanoborohydride. The residual activity versus time data were fitted to a single exponential with an offset to account for the activity remaining after prolonged reaction. The rate of methylation of DGD-PMP versus pH yields a pK_a values of 8.8 (Table 1). A fit of the offset values versus pH yields a pK_a value of 8.3 for DGD-PMP.

After exhaustive methylation, 7% of the original activity was regained by reconstituting apoenzyme with PLP. The CD spectrum of the reconstituted enzyme has no peak at 410 or 330 nm as does the native enzyme, but shows a small one at ~350 nm.

Spectrophotometric pH Titration of DGD-PLP. Absorption spectra of DGD-PLP at various pH values are shown in Figure 5A. These data were analyzed globally with Specfit. The spectra do not show an isosbestic point, suggesting the presence of multiple ionizations. The data fit best to a model with three ionizations. Fits to models for one and two ionizations give substantially larger sum-of-the-squares deviations and, for the two ionization fit, chemically unreasonable fitted spectra for some of the individual species. The pK_a values obtained from fits to three ionizations are 6.0, 7.3, and 8.9 (Table 1). These values are averages from three independent titrations. The fitted absorbance spectra for the four different ionization states of DGD-PLP are shown in Figure 5B. A titration of free PLP was performed under indentical conditions (data not shown). The pK_a values obtained are 5.4 ± 0.2, 7.9 ± 0.1, and 9.5 ± 0.5. These are very different from those observed in the DGD-PLP titration and serve to rule out the possibility that free coenzyme contributes to the changes observed with the enzyme.

Log-normal deconvolution of the four spectra obtained from global analysis into their component absorption bands (*5*) provided the band positions and percentages given in Table 2. It is noteworthy that substantial amounts of both ketoenamine (~410 nm) and enolimine (~330 nm) tautomers (Scheme 2) are present in the low and high pH forms of DGD-PLP.

Fluorescence pH Titration of IANBD-Labeled DGD-PLP. DGD-PLP was reacted with IANBD, a fluorescent probe sensitive to environment polarity, and the excess reagent was removed. Fluorescence emission spectra versus pH were collected for the labeled enzyme and analyzed globally. Three ionizations were indicated by residual values and the fitted spectra. The fitted pK_a values are 7.4, 8.5, and 8.8 (Table 1).

Fluorescence pH Titration DGD-PMP. DGD-PMP fluoresces in the range of 350−450 nm when excited at 330 nm. Emission spectra versus pH were collected and analyzed globally. Two ionizations were indicated by residual values and the fitted spectra. The first is 7.8 while the second is 8.3 (Table 1).

DISCUSSION

The pH dependence of catalysis for only a few pyridoxal phosphate-dependent enzymes has been well-studied in efforts to elucidate ionizations controlling their activities. The studies by Velick and Vavra (*8*), Kiick and Cook (*9*), and

Table 1: pK_a Values Associated with Dialkylglycine Decarboxylase[a]

	pK_a 1	pK_a 2	pK_a 3	pK_a 4	pK_a 5	pK_a 6	pH-independent limits
k_{cat}	5.9 ± 0.1				8.7 ± 0.1		17.8 ± 0.4 s^{-1}
k_{cat}/K_{AIB}		7.3 ± 0.1			9.1 ± 0.1		(1.1 ± 0.1) × 10^4 M^{-1} s^{-1}
k_{cat}/K_{pyr}			7.8 ± 0.1				(3.3 ± 0.2) × 10^5 M^{-1} s^{-1}
$1/K_{AIB}$		7.5 ± 0.1					
$1/K_{is}$	6.0 ± 0.2	7.5 ± 0.2					10.0 ± 0.5 mM
K_{PLP}	5.4 ± 0.3	7.6 ± 0.2					2.4 ± 0.1 μM
K_d for K^+					8.8 ± 0.1		0.28 ± 0.01 mM
							28 ± 4 mM
amplitude 1 for DTNB				8.2 ± 0.15	8.7 ± 0.3		
amplitude 2 for DTNB					8.80 ± 0.05		
DGD-PMP methylation rate					8.8 ± 0.2		0.14 ± 0.01 min^{-1}
							0.41 ± 0.01 min^{-1}
DGD-PMP methylation offset				8.3 ± 0.1			
DGD-PMP fluorescence pH titration			7.8 ± 0.1	8.3 ± 0.4			
DGD-PLP spectrophotometric pH titration	6.0 ± 0.2	7.3 ± 0.1			8.9 ± 0.1		
IANBD-labeled DGD-PLP fluorescence pH titration		7.4 ± 0.1		8.5 ± 0.1	8.8 ± 0.2		
AIB titration[b]						10.10 ± 0.01	

[a] Initial rate conditions: 100 mM buffer, 100 mM dipotassium succinate, 10 mM disodium succinate, 500 μM PLP, 200 μM NADPH, 1 units/mL 2° ADH, varying concentrations of AIB and pyruvate, 25°C. K_{PLP} was determined under identical conditions except: (1) the PLP concentration was varied, (2) reactions were preincubated for 1 h at 25 °C, (3) fixed concentrations of AIB (40 mM) and pyruvate (2 mM) were used, and (4) reactions were initiated by the addition of AIB. K_{is} and K_{ii} correspond to competitive and uncompetitive inhibition constants, respectively. [b] Titrations were performed in the presence of 100 mM dipotassium succinate.

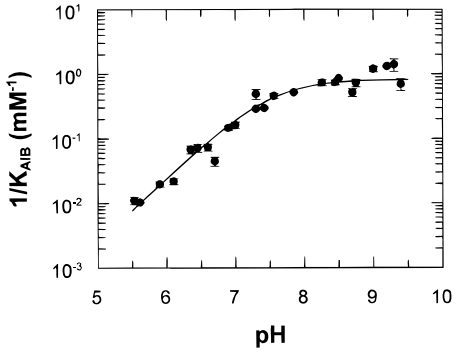

FIGURE 3: The pH dependence of $1/K_{AIB}$. The pK_a value is 7.5 ± 0.1, identical, within error, to that obtained from k_{cat}/K_{AIB}, K_{is}, K_{PLP}, and absorbance and fluorescence titrations.

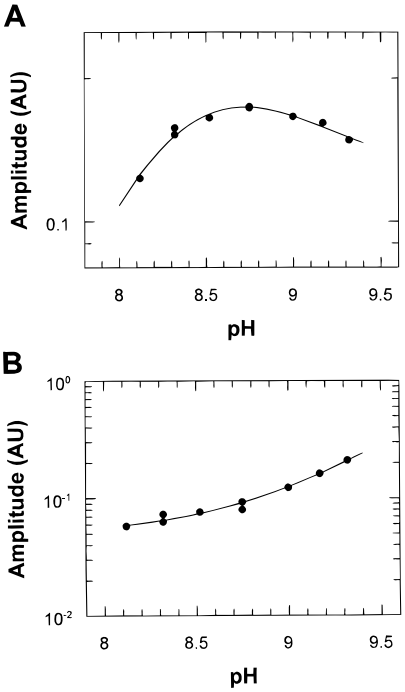

FIGURE 4: (A) The pH dependence of the amplitude of the fast phase in the reaction of DGD-PLP with DTNB. DGD-PLP exists in solution as a mixture of two conformers. This reaction probes the conformational distribution of the enzyme (*4*). The pK_a values obtained are 8.2 ± 0.15 and 8.7 ± 0.3. (B) The pH dependence of the amplitude of the slow phase in the reaction of DGD-PLP with DTNB. The pK_a value is 8.80 ± 0.05. Note the complimentary decrease in the fast phase amplitude and the increase in the slow phase amplitude with the pK_a of ~8.8.

Gloss and Kirsch (*10*) provide detailed mechanistic information for the reaction catalyzed by aspartate aminotransferase. Other notable examples include the studies by Kiick and Phillips on tryptophan indole-lyase (*11*) and tyrosine phenol-lyase (*12*), by Koushik et al. on kynureininase (*13*), by Tai et al. on O-acetylserine sulfhydrylase (*14*), and by Chen and Metzler on cat brain glutamate decarboxylase (*15*).

The following discussion attempts to assign the pK_a values observed in the pH dependence of the steady-state kinetic parameters for the DGD-catalyzed reaction between AIB and pyruvate. Extra-kinetic information derived from the pH dependence of DTNB and methylation reactions, and from spectroscopic pH titrations of DGD in its PLP and PMP forms, provides supporting evidence for the assignments.

Ping-Pong Kinetic Mechanism. Previous work by Honma's and Dempsey's groups (*6, 7*) suggests that DGD follows a ping-pong bi bi kinetic mechanism and demonstrates substrate inhibition by pyruvate. The data in Figure 1 are consistent with their findings. The high concentrations of pyruvate employed here exaggerate the substrate inhibition by pyruvate previously observed by these authors. This is most evident in Figure 1B where the initial rates clearly decrease at high pyruvate concentrations. Ping-pong kinetics are evidenced by the parallel double-reciprocal lines at low pyruvate concentrations. The ping-pong nature of the reaction is independently confirmed by the facts that AIB and pyruvate (each in the absence of the other) react with DGD-PLP and DGD-PMP, respectively, and that the steady-state kinetic parameters can be accounted for by pre-steady-state half-reaction data and a ping-pong kinetic mechanism (*4*).

AIB Is Not a Sticky Substrate. The absorbance and fluorescence pH titrations of DGD-PLP and IANBD-labeled

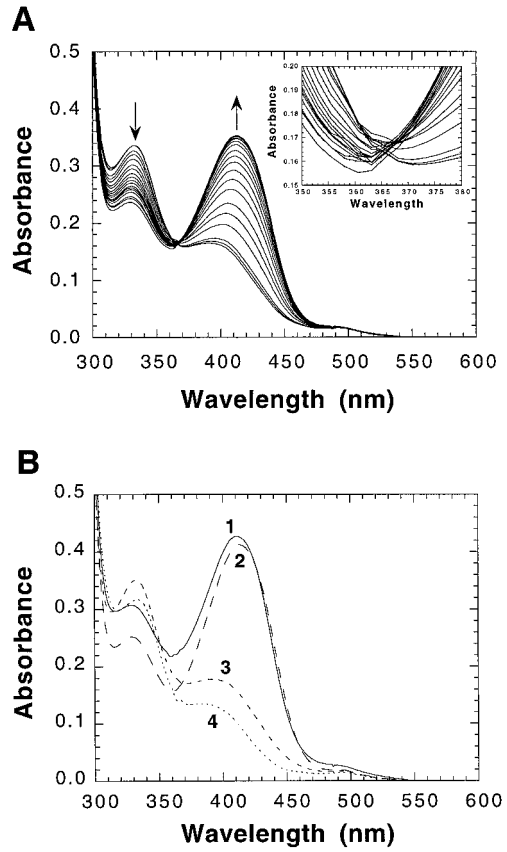

FIGURE 5: (A) Coenzyme absorbance spectra obtained in the pH titration of DGD-PLP. The arrows indicate the direction of change with decreasing pH. (B) Calculated spectra for the four ionization states corresponding to the three pK_a's (6.0 ± 0.2, 7.3 ± 0.1, and 8.9 ± 0.1). The spectra and pK_a's were obtained through global analysis of the raw data with Specfit.

Table 2: Lognormal Deconvolution of Absorbance Spectra for the Four Species Observed in the pH Titration of DGD-PLP[a]

	ionization state			
absorption band	1 high pH	2	3	4 low pH
ketoenamine				
position (nm)	401	405	409	411
percentage of total	20%	26%	63%	50%
dipolar				
position (nm)	371	370		364
percentage of total	13%	12%		14%
enolimine				
position (nm)	330	327	326	325
percentage of total	66%	61%	36%	35%

[a] The sum of five lognormal curves (*5*) was used to fit ionization states 1, 2, and 4 while four were used to fit ionization state 3. A band at 487−492 nm is present in all four species. This band contributes 1.5% or less to each spectrum. The origin of this band is not clear, although it was also seen in tryptophanase (*23*). It is not included in the table. The protein peak at ∼280 nm is also not reported.

DGD-PLP, respectively, both yield the pK_a value of ∼7.4 (Table 1). The pH dependence of the pyruvate K_{is} yields a similar value (∼7.6). The decrease in K_{is} at low pH due to this pK_a presumably originates from the tighter binding of pyruvate to DGD-PLP in the ketoenamine form, as occurs in the binding of keto acid substrates and dicarboxylic inhibitors to the PLP form of aspartate aminotransferase (*8*−*10*).

The above pK_a values are true thermodynamic ones since all species involved are at equilibrium. The pH dependence

Scheme 2

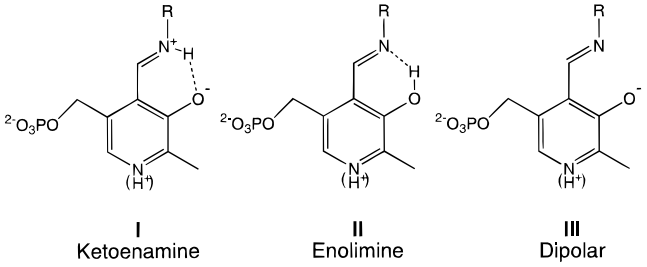

of the kinetic parameter k_{cat}/K_{AIB} yields a similar pK_a value of ∼7.4. The agreement between the thermodynamic and kinetic pK_a values strongly suggests that the binding of AIB to DGD-PLP is rapid and at equilibrium with respect to subsequent steps; that is, AIB is not a sticky substrate (*16*). Pre-steady-state data also suggest that external aldimine formation is rapid with both AIB and L-alanine (Zhou, X., and Toney, M. D., manuscript in preparation). Such is also the case with reactions of amino acids with the PLP form of aspartate aminotransferase, although this is not always so for PLP-dependent enzymes (*17, 18*).

The pH dependence of $1/K_M$, like that of k_{cat}/K_M, reports on ionizations of the free enzyme and free substrate *only in a rapid equilibrium kinetic mechanism (i.e., when substrate is not sticky)* (*19*). The pK_a of ∼7.5 observed in the pH dependence of $1/K_{AIB}$ (Table 1) matches those discussed above for pH titrations and for k_{cat}/K_{AIB}. The expression for K_M in general equations for a ping-pong kinetic mechanism contains rate constants from both half-reactions, while the k_{cat}/K_M expressions contain rate constants only from the cognate half-reaction (*8*). Given the above agreement in pK_a values between $1/K_{AIB}$ and k_{cat}/K_{AIB}, it is very likely that rate constants solely from the decarboxylation half-reaction contribute significantly to K_{AIB}, and, by extension, that the decarboxylation step (or possibly a conformational change preceding it) fully limits the rate of the overall catalytic cycle since AIB binding is rapid. Pre-steady-state data corroborate this conclusion (*4, 20*; Zhou and Toney, manuscript in preparation).

Phosphate Ionization in DGD-PLP. The ionization with a pK_a value of ∼6 is observed in the pH dependence of several parameters: k_{cat} (which reports on ionizations of the external aldimine intermediate since decarboxylation is rate-limiting), K_{is}, DGD-PLP absorbance titration, and K_{PLP}. The presence of this ionization in parameters that report on diverse forms of the enzyme (e.g., AIB external aldimine, free DGD-PLP) suggests that it is not associated with a group interacting with the substrate. Its presence in K_{PLP} suggests that the phosphate ester of the coenzyme is a likely origin of this pK_a. Schnackerz et al. (*21*) observed a similar pK_a for the coenzyme phosphate group in D-serine dehydratase.

Conformational Change Interconverting Fast and Slow Enzyme Forms. Zhou and Toney (*4*) demonstrated that DGD-PLP at pH 8.2 exists as a mixture of fast (∼60%) and slow (∼40%) enzyme conformations when potassium is bound. The conformational equilibrium was shown to depend on the identity of the alkali metal ion bound near the active site; the sodium enzyme form is nearly inactive and only one form is observed kinetically.

The ionization with a pK_a value of ∼8.8 (Table 1) is best ascribed to a group controlling the interconversion of the

fast and slow reacting conformations of DGD-PLP. This is strongly supported by the observation of this pK_a in the pH dependence of the amplitudes of the two kinetic processes observed in the reaction of DGD-PLP with DTNB. The DTNB reaction is sensitive to the conformational equilibrium between fast and slow forms, with the catalytically more active form reacting faster with DTNB (*4*). The pK_a of ~8.8 causes a decrease in the fast phase amplitude and a complementary increase in the slow phase amplitude in the DTNB reaction (Figure 4), suggesting a conversion from fast to slow reacting enzyme forms as pH increases. This is consistent with the decrease in k_{cat} at high pH, which is controlled by this pK_a.

The presence of a pK_a of 8.8 in the pH profile for potassium K_d lends further weight to the assignment of this ionization to a conformational change. Alkali metal ion size alters the conformational distribution (*4*), and thus ionizations controlling the conformational distribution are expected to modulate metal ion binding.

The pH titration of IANBD-labeled DGD-PLP fluorescence should be sensitive to conformational changes since this probe is highly sensitive to the environment. The cysteine that reacts rapidly with DTNB was presumably labeled since a small fraction (~5%) of the total enzyme was modified. The observation of the pK_a of ~7.4 in the IANBD fluorescence suggests that a small change in tertiary structure is associated with this ionization. Similarly, the pK_a of ~8.3 in both the amplitude of the fast phase of the DTNB reaction and the IANBD fluorescence titration suggests a small, catalytically insignificant structural change since it is not seen in any steady-state parameters for DGD-PLP. The pK_a of 8.8 is clearly seen in the IANBD fluorescence titration, as it is in the DGD-PLP absorbance titration. This further strengthens the argument that this ionization is associated with a kinetically significant conformational change between the previously characterized fast and slow forms of the enzyme.

There is no evidence to support an assignment of the pK_a of 8.8 to a specific group. One can speculate that it is in the alkali metal ion binding site near the active site, since DGD-PLP has been shown to undergo a metal ion size-dependent conformational change (*3*). This binding site contains two histidine residues, one aspartate residue, and one water molecule. One can rule out the pyridine nitrogen of PLP since Scott et al. (*22*) have shown this pK_a to be immeasurably high in the structurally homologous active site of aspartate aminotransferase. Assignments of this ionization to active site residues meet with additional difficulty; it is present in the free enzyme (k_{cat}/K_{AIB}, spectral titrations), the enzyme−substrate complex (k_{cat}), and the PMP enzyme form (methylation rate) (see Table 1), which are unlikely to present similar electrostatic environments in the active site.

Ionizations in DGD-PMP. The PMP form of DGD displays a pK_a of 7.8 in both k_{cat}/K_{pyr} and the fluorescence pH titration. This is unlikely to be either the PMP amino group or the ϵ-amino group of Lys272 since this ionization is not seen in the pH profile for DGD-PMP methylation (Table 1). Rather, it is likely an active site residue interacting with the coenzyme, whose electrostatic environment substantially changes between the PLP and PMP enzyme forms (possibly Glu210, see below). This ionization is not observed in any parameter associated with DGD-PLP.

The pK_a of 8.3 observed in the fluorescence titration of DGD-PMP and the methylation offset might originate in the conformational change assigned above to the pK_a of 8.8 in DGD-PLP. This suggestion is based on the fact that this ionization affects the methylation offset (i.e., the amount of enzyme that remains unreacted over long periods) and not the rate, as would be expected if either PMP or Lys272 ionized. The methylation rate is controlled by a pK_a of 8.8. The low activity regained on reconstitutiuon of methylated enzyme with PLP argues that Lys272, not PMP, ionizes with this pK_a, which is fortuitously coincident with that assigned to the conformational change in DGD-PLP. These assignments should be taken with caution due to the tenuous nature of the evidence supporting them.

Tautomeric Equilibria in the High and Low pH Forms of DGD-PLP. Three ionizations were observed in the DGD-PLP coenzyme absorbance spectra taken as a function of pH. This is not unprecedented. Metzler et al. (*23*), for example, found that tryptophanase has at least two ionizations observable by coenzyme absorbance.

Table 2 contains the positions of the component bands, obtained by log-normal deconvolution, of the spectra for the four ionization states and their percentages of the total coenzyme species present. The largest spectral change occurs in the second ionization, which leads from state 2 to 3 (Figure 5B). This ionization also has a pK_a value that is similar to that observed in absorbance titrations of aspartate aminotransferase, where the color change has been assigned to deprotonation of the aldimine nitrogen (*10*), leading from the ketoenamine to the dipolar form (Scheme 2). Like in aspartate aminotransferase, the second ionization in DGD-PLP greatly affects the affinity of DGD-PLP for ligands (Table 1). Thus, one might a priori expect it also to be the protonation/deprotonation of the internal aldimine nitrogen. This is clearly not possible since both states 2 and 3 contain substantial amounts of the ketoenamine tautomer (**I**, Scheme 1) absorbing at ~410 nm. The dipolar tautomer (**II**), on the other hand, disappears from the spectrum in state 3 (Table 1).

The presence of both ketoenamine and enolimine tautomers is common in PLP-dependent enzymes (for example, see refs *23*−*29*). It may be that aspartate aminotransferase, with its simple transition between ketoenamine and dipolar species on loss of a proton in pH titrations, is the exception rather than the rule.

Scott et al. (*22*) have shown that the pK_a for the pyridine nitrogen of 6-fluoroPLP is reduced by approximately 5 units relative to PLP. They also measured a pyridine nitrogen pK_a of ~8.2 for 6-fluoroPLP in aspartate aminotransferase. Thus, one can estimate that the binuclear Asp222-pyridine nitrogen base has a pK_a value of ~13 in native aspartate aminotransferase. This is in agreement with the pH studies performed by Gloss and Kirsch (*10*). The high homology between the active site structure of aspartate aminotransferase and DGD near the pyridine nitrogen (*2*) strongly supports the assumption that the pyridine nitrogen pK_a in DGD is so high as to be experimentally inaccessible. Given that it is unreasonable to assign the ionization with a pK_a of ~7.4 to either the aldimine or pyridine nitrogen on the basis of the above, one must seek an alternative assignment for the group responsible.

DGD-PLP emits flourescence only at ~415 nm (increasing with increasing pH) when excited at 330 nm, and at ~500

nm (much lower intensity) when excited at 410 nm. Other examples are known where PLP-dependent enzymes give ~420 nm fluorescence from ~330 nm absorption bands (e.g., *27*−*29*). The structure giving ~420 nm fluorescence has generally been assigned to an adduct formed between the internal aldimine and a nucleophile at high pH, rather than to a free aldimine species (e.g., refs *28*, *29*). This assignment appears unwarranted as it is based simply on the observation that PMP and aldimine adducts fluoresce at ~415 nm.

Honikel and Madsen (*30*) have very clearly demonstrated that Schiff bases of PLP with amines in various solvents can emit solely at either ~430 or ~510 nm, or a combination of both wavelengths depending on the polarity and acidity of the solvent. Acid promotes the ~510 nm emission at the expense of the ~430 nm emission. Subsequently, Segura et al. (*31*) demonstrated that emission of ~430 nm versus ~510 nm fluorescence from PLP Schiff bases excited at ~330 nm is determined by a competition between (1) proton transfer from the 3′-hydroxyl group of the enolimine to the aldimine nitrogen of the ketoenamine in the singlet excited state; and (2) radiative decay of the excited state to the ground state. That is, excitation of an enolimine tautomer of a PLP Schiff base can lead to emission at either ~430 nm (from the enolimine) or ~510 nm (from the ketoenamine), depending on the relative rates of proton transfer and radiative decay in the excited state. Thus, the ~420 nm fluorescence from DGD-PLP (and other enzymes) likely results directly from the excited state of the enolimine tautomer of the Schiff base before it has tautomerized to the ketoenamine excited state.

Segura et al. also show that the rate of proton transfer in the excited state depends strongly on the protonation state of the pyridine nitrogen, with the N-protonated Schiff bases giving faster proton transfer in the excited state. Analogously, the 3′-hydroxyl of PLP is 4.5 pH units more acidic when the ring is N-protonated (*32*). This provides a clear explanation for the results of Honikel and Madsen showing greater ~510 nm emission (when excited at ~330 nm) in acidic versus neutral solvents. Thus, one might expect from these results that the pyridine nitrogen in DGD-PLP is not fully protonated as is usually assumed for PLP-dependent enzymes having an aspartate residue interacting with the pyridine nitrogen.

An explanation that accounts for the observations with DGD-PLP and other enzymes is that the ionization observed in pH titrations of coenzyme absorbance is not associated with any functional group on the Schiff base itself. Rather, it is an active site residue in close proximity to the coenzyme whose ionization alters the ratio between the ketoenamine and enolimine tautomers through electrostatic effects. Chu and Metzler proposed the same for glutamate decarboxylase (*33*). It is important to note at this point that the absorbance spectra of several PLP-dependent enzymes is invariant with pH (e.g., refs *24*, *34*), suggesting that it is common for PLP Schiff bases in active sites not to ionize. This observation also weighs against the possibility that the ~330 nm absorbing species in these enzymes is a deprotonated form in which the Schiff base is not coplanar to the pyridine ring, although this cannot be rigorously excluded for DGD.

A good candidate for an ionizing residue that affects tautomer equilibria in DGD is Glu210. This amino acid is strictly conserved in the evolutionary subgroup II of aminotransferases, yet has no obvious mechanistic role when aspartate aminotransferase is used as a mechanistic prototype. It is located in the lower part of the active site near the 2′-methyl group of PLP (*2*).

The suggestion that the aldimine nitrogen does not ionize poses a mechanistic problem since protonated amino acids predominate at physiological pH, and a productive Michaelis complex is one where a single proton is shared between the aldimine and substrate nitrogens (*10*). This can be resolved if one assumes that Glu210 (or whichever residue is responsible for the ionization) acts as a proton acceptor from the amino acid substrate in the initial Michaelis complex where two protons are present. This would have to occur through water molecules located above Glu210, which are observed in the X-ray structure (*2*). This hypothesis is testable by mutagenesis. Taking a step further with this line of reasoning, one might imagine that the enolimine tautomer is the reactive one for binding protonated amino acid substrate since its aldimine is formally uncharged.

CONCLUSIONS

Dialkylglycine decarboxylase shows five observable, kinetically significant ionizations. The following tentative assignments for these have been made: pK_a1 (~6.0), the phosphate ester of DGD-PLP; pK_a2 (~7.4), an active site residue (possibly Glu210) in DGD-PLP; pK_a3 (~7.8), an active site residue (possibly Glu210) in DGD-PMP; pK_a4 (~8.3), possibly a conformational change in DGD-PMP; pK_a5 (~8.8), a conformational change in DGD-PLP; pK_a5′ (~8.8), Lys272 ϵ-amino group in DGD-PMP.

An analysis of enzyme and model Schiff base fluorescence spectra lead to the suggestion that, in general, the 330 nm absorbing species in PLP-dependent enzymes is not a covalent adduct of a Schiff base with a nucleophile; rather it is the enolimine tautomer of the internal aldmine. The observation of ketoenamine and enolimine tautomers in all four ionization states observed in pH titrations of DGD-PLP coenzyme absorbance demonstrates that the kinetically significant ionization with a pK_a of ~7.4 cannot be deprotonation of the aldimine nitrogen. It must be an active site residue (suggested to be Glu210) whose ionization affects the ketoenamine/enolimine tautomeric ratio.

REFERENCES

1. Toney, M. D., Hohenester, E., Cowan, S. W., and Jansonius, J. N. (1993) *Science 261*, 756−759.
2. Toney, M. D., Hohenester, E., Keller, J. W., and Jansonius, J. (1995) *J. Mol. Biol. 245*, 151−179.
3. Hohenester, E., Keller, J. W., and Jansonius, J. N. (1994) *Biochemistry 33*, 13561−13570.
4. Zhou, X., Kay, S., and Toney, M. D. (1998) *Biochemistry 37*, 5761−5769.
5. Metzler, C. M., and Metzler, D. E. (1987) *Anal. Biochem. 166*, 313−327.
6. Honma, M., and Shimomura, T. (1974) *Agric. Biol. Chem. 38I*, 953−958.
7. Lamartiniere, C. A., Itoh, H., and Dempsey, W. B. (1971) *Biochemistry 10*, 4783−4788.
8. Velick, S. F., and Vavra, J. (1962) *J. Biol. Chem. 237*, 2109−2122.
9. Kiick, D. M., and Cook, P. F. (1983) *Biochemistry 22*, 375−382.
10. Gloss, L. M., and Kirsch J. F. (1995) *Biochemistry 34*, 3999−4007.
11. Kiick, D. M., and Phillips, R. S. (1988) *Biochemistry 27*, 7339−7344.

12. Kiick, D. M., and Phillips, R. S. (1988) *Biochemistry 27*, 7333−7338.
13. Koushik, S. V., Moore, J. A., Sundararaju, B., and Phillips, R. S. (1998) *Biochemistry 37*, 1376−1382.
14. Tai, C.-H., Nalabolu, S. R., Simmons, J. W., Jacobson, T. M., and Cook, P. F. (1995) *Biochemistry 34*, 12311−12322.
15. Chen, W.-C., and Metzler, D. E. (1994) *Anal. Biochem. 313*, 287−295.
16. Cleland, W. W. (1977) *Adv. Enzymol. 45*, 297−387.
17. Abell, L. M., and O'Leary, M. H. (1988) *Biochemistry 27*, 3325−3332.
18. Abell, L. M., and O'Leary, M. H. (1988) *Biochemistry 27*, 5927−5933.
19. Fersht, A. (1985) *Enzyme Structure and Mechanism*, p 161, Freeman, NY.
20. Sun, S., Bagdassarian, C., and Toney, M. D. (1998) *Biochemistry 37*, 3876−3885.
21. Schnackerz, K. D., Feldman, K., and Hull, W. E. (1979) *Biochemistry 18*, 1536−1539.
22. Scott, R. D., Chang, Y.-C., Graves, D. J., and Metzler, D. E. (1985) *Biochemistry 24*, 7668−7681.
23. Metzler, C. M., Viswanath, R., and Metzler, D. E. (1991) *J. Biol. Chem. 266*, 9374−9381.
24. Marino, G., Nitti, G., Arnone, M. I., Sannia, G., Gambacorta, A., and De Rosa, M. (1988) *J. Biol. Chem. 263*, 12305−12309.
25. Osterman, A. L., Brooks, H. B., Rizo, J., and Phillips, M. (1997) *Biochemistry 36*, 4558−4567.
26. Gong, J., Hunter, G. A., and Ferreira, G. C. (1998) *Biochemistry 37*, 3509−3517.
27. Isom, H. C., and DeMoss, R. D. (1975) *Biochemistry 14*, 4291−4297.
28. Misono, H., and Soda, K. (1997) *J. Biochem. 82*, 535−543.
29. Hayashi, H., Mizuguchi, H., and Kagamiyama, H. (1993) *Biochemistry 32*, 812−818.
30. Honikel, K. O., and Madsen, N. B. (1972) *J. Biol. Chem. 247*, 1057−1064.
31. Segura, M. A. V., Donoso, J., Munoz, F., Blanco, F. G., Del Vado, M. A. G., and Echevarria, G. (1994) *Photochem. Photobiol. 60*, 399−404.
32. Christen, P., and Metzler, D. E., Eds. (1986) *Transaminases*, Chapter 2, Wiley, NY.
33. Chu, W.-C., and Metzler, D. E. (1994) *Arch. Biochem. Biophys. 313*, 287−295.
34. Cook, P. F., Hara, S., Nalabolu, S., and Schnackerz, K. (1992) *Biochemistry 31*, 2298−2303.

BI981455S